

Effect of Cutting Forces on the Form-Shaping Motion in Robotic Milling

Ha Thanh Hai

¹School of Mechanical Engineering, Hanoi University of Science and Technology

Corresponding Author: Ha Thanh Hai

ABSTRACT: This article presents analysis of dynamics of robots in milling process. A number of factors affects to dynamics model, as well as cutting, form-shaping motion of the robot. Among these factors, cutting forces generating in machining process are strongly variable factor, because of material heterogeneity, depth of cut, machining geometrical surface, etc. Indeed, if cutting force values are constant, the directions of cutting force vectors always change during cutting process. The cutting forces affect to robot's motion, it is hard to determine precisely cutting force values. This paper presents analysis of cutting forces by building computing formulas, deriving and solving differential equations of motion of the robot in milling process. The program of computing and solving the differential equations of motion enables evaluating of the effects of the cutting forces and its calculating errors to form-shaping motion of the robot. The results create a premise to study calibration and elimination effects of cutting force changes with respect to form-shaping motion of robots in milling process.

KEYWORDS: cutting force, robotic miling, form-shaping motion.

Date of Submission: 07-07-2019

Date of Acceptance: 25-07-2019

I. INTRODUCTION

Potentials of applying robot in machining process are huge due to the advantages, to compare with conventional machine tools and CNC machines [1-4]. The most disadvantage of machining using robots is hard to reach to high absolute accuracy. [3-5] presented a number of factors that affect to capability of matching machining accuracy of robots, such as inaccuracy of deriving kinematics and dynamics models, less of structure stiffness, vibration under acting forces, etc. These causes lead to errors of dynamics model and differential equations of motion. This affects to errors in form-shaping motion and machining accuracy. However, the factors that cause errors of kinematic and dynamic parameters, such as lengths of links, masses, center of masses, inertial tensors, etc., can be eliminated or minimized by calibrating.

The cutting forces applying on the cutter in machining process are unable to be determined precisely. The cutting forces depend on material, depth of cut, cutting speed, etc. When these parameters are constants, the cutting forces values can be evaluated as a constant, but the directions of cutting forces always change due to the complicated geometrical machining surface. In addition, the cutting forces act on the end-effector that is the last link of the kinematic chain, which consists of a large number of joints and links. As a result, computing and expressing the cutting forces in the differential equation of motions are complicated.

[6,7] mentioned analysis of cutting forces, as well as loads on robots in milling processes. [8] introduced a method of trajectory design and analysis of robots in machining. The general method to derive the differential equations of motion of the robots is showed in [9,10]. [10] proposed adjusting cutting forces in machine, base on algorithm of inverse kinematic control of robot in milling process. [11-16] presented methods to determine cutting forces in milling process.

The problems of dynamics and controls of robots in machining processes in general, and in high accurate machining such as milling, grinding, etc., to form and shape part surfaces are still challenges so far.

The paper presents deriving of the differential equations of motion of the robot in milling process. The homogeneous transformation matrices are utilized to compute and express the kinematic and dynamic

parameters and terms. Especially, computing the general forces of non-gravitational forces, which mean cutting forces in this paper, are hard. As mentioned above, the cutting forces act on the end-effector of the kinematic chain, which consists of a large number of joints and links, and directions, values of cutting forces vary by time. By using the transformation coordinate matrices, formulating expressions of cutting forces and dynamic parameters and terms in the differential equations of motion are automatic performed by a computer program.

The solution of the differential equations of motion of a specific example is carried out. Suppose that calculating cutting force values exists errors, the results of computing and simulating programs enable to evaluate effect of cutting force errors to the form-shaping motion of the robot. The results provides the basic to conduct next studies, to minimize or eliminate cutting force errors to form-shaping motion of the robot.

The paper consists of 6 parts. After the introduction part, part 2 and part 4 present kinematic and dynamic modelling respectively. Part 4 shows the cutting force model, which bases on the empirical formulas and calculating cutting forces. Part 5 presents computations and solutions of the dynamic equations of a specific robot milling along a tool path. Assume that manipulating requirements are defined, such as workpiece material, cutter, tool path, cutting process parameters, estimated average values of cutting forces. The solution of dynamic problem is carried out to determine form-shaping motion and driving torques. The numerical computing results enable to evaluate the effects of cutting forces and errors of estimating cutting force values to the form-shaping motion. Part 6 gives conclusion of the study and future works.

II. ROBOT KINEMATICS

Figure 1 shows presentation of the robot that has a serial structure and 6 degrees of freedom. The method of transformation coordinates and homogeneous transformation matrices are applied to compute and derive kinematic model of the robot.

Table 1 presents notations of the links, frames, homogeneous transformation matrices.

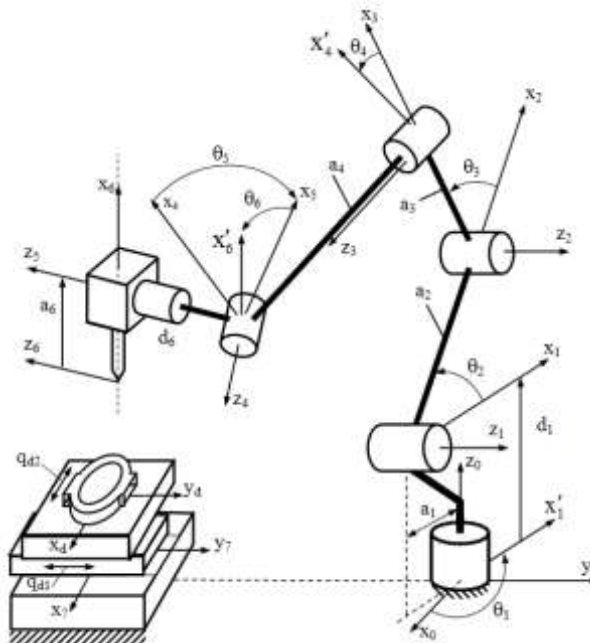


Figure 1. Kinematics diagram of the machining robot

Table 1: Notation of links, frames and DH parameters of the robot

Link	Frames	Kinematic parameters				Transformation matrix
		θ_i	d_i	a_i	α_i	
LK0	$O_0x_0y_0z_0$	0	0	0	0	
LK1	$O_1x_1y_1z_1$	θ_1	d_1	a_1	α_1	0A_1
...
LK6	$O_6x_6y_6z_6$	θ_6	d_6	a_6	α_6	5A_6
E	$O_ExEyEzE$	θ_E	d_E	a_E	α_E	6A_E

Here, LK0 is the fixed link or the fixed base. The frame $O_0x_0y_0z_0$ is attached to the fixed base, called the world frame. LK6 is the end-effector, E is the end-effector point, which is attached on the tool frame, called the tool trihedron $O_ExEyEzE$, featured by geometric shape of cutting tooth. The position of the tool

trihedron $O_E X_E Y_E Z_E$ with respect to the operational frame $O_6 X_6 Y_6 Z_6$ is determined by constant parameters, that means $\theta_E, d_E, a_E, \alpha_E$ are constants due to this two frames are fixed on the end-effector LK6.

The joint variables are notated (1):

$$q = [q_1, \dots, q_6]^T = [\theta_1, \dots, \theta_6]^T \tag{1}$$

Table 2 shows notations of the clamping table, the clamping frames, the workpiece frames, the workpiece surface trihedrons [8]. In which, the workpiece surface trihedron is determined by geometric shape of workpiece surface, the origin O_i is on the tool path. The position and orientation of the workpiece trihedron are determined by ${}^d x_{fi}, {}^d y_{fi}, {}^d z_{fi}, {}^d \alpha_{fi}, {}^d \beta_{fi}, {}^d \eta_{fi}$, notated (2).

Table 2: Notation of links, frames and DH parameters of the clamping table

Links	Frames	Kinematic parameters						Transformation matrice
		x_i	y_i	z_i	α_i	β_i	η_i	
LK0	$O_0 X_0 Y_0 Z_0$	0	0	0	0	0	0	
LKB	$O_b X_b Y_b Z_b$	x_b	y_b	z_b	α_b	β_b	η_b	${}^0 A_b$
LKD	$O_d X_d Y_d Z_d$	x_d	y_d	z_d	α_d	β_d	η_d	${}^b A_d$
O_{fi}	$O_{fi} X_{fi} Y_{fi} Z_{fi}$	${}^d x_{fi}$	${}^d y_{fi}$	${}^d z_{fi}$	${}^d \alpha_{fi}$	${}^d \beta_{fi}$	${}^d \eta_{fi}$	${}^d A_{fi}$
E	$O_E X_E Y_E Z_E$	${}^d x_E$	${}^d y_E$	${}^d z_E$	${}^d \alpha_E$	${}^d \beta_E$	${}^d \eta_E$	${}^d A_E$

$${}^d p_{fi} = [{}^d x_{fi}, {}^d y_{fi}, {}^d z_{fi}, {}^d \alpha_{fi}, {}^d \beta_{fi}, {}^d \eta_{fi}]^T \tag{2}$$

From parameters (2), position of the workpiece trihedron at a point on the workpiece surface, along the tool path, with respect to the workpiece frame that is expressed by (3).

$${}^d A_{fi} ({}^d p_{fi}) = \begin{bmatrix} {}^d C_{fi} ({}^d \alpha_{fi}, {}^d \beta_{fi}, {}^d \eta_{fi}) & {}^d r_{fi} ({}^d x_{fi}, {}^d y_{fi}, {}^d z_{fi}) \\ 0^T & 1 \end{bmatrix} \tag{3}$$

The parameters that express the position and orientation of the tool trihedron with respect to the workpiece frame are ${}^d x_E, {}^d y_E, {}^d z_E, {}^d \alpha_E, {}^d \beta_E, {}^d \eta_E$, notated (4).

$$p = {}^d p_E = [{}^d x_E, {}^d y_E, {}^d z_E, {}^d \alpha_E, {}^d \beta_E, {}^d \eta_E]^T \tag{4}$$

The parameters (4) is called operational coordinates. From the parameters (4), the position of the tool trihedron [8] with respect to the workpiece frame is expressed by matrix (5):

$${}^d A_E ({}^d p_E) = \begin{bmatrix} {}^d C_E ({}^d \alpha_E, {}^d \beta_E, {}^d \eta_E) & {}^d r_E ({}^d x_E, {}^d y_E, {}^d z_E) \\ 0^T & 1 \end{bmatrix} \tag{5}$$

The parameters of the Table 2 are constants, because the workpiece is fixed in milling process.

Position and orientation of the tool with respect to the world frame are determined by the two kinematic chains (6), (7):

$${}^0 A_E ({}^d p_E) = {}^0 A_d {}^d A_E ({}^d p_E) = \begin{bmatrix} {}^0 C_E ({}^d \alpha_E, {}^d \beta_E, {}^d \eta_E) & {}^0 r_E ({}^d x_E, {}^d y_E, {}^d z_E) \\ 0^T & 1 \end{bmatrix} \tag{6}$$

$${}^0 A_E (q) = {}^0 A_1 (q_1) {}^1 A_2 (q_2) \dots {}^5 A_6 (q_6) {}^6 A_E \tag{7}$$

From (6), (7), obtained kinematic equation in matrix form (8),

$${}^0 A_d {}^d A_E ({}^d p_E) = {}^0 A_1 (q_1) {}^1 A_2 (q_2) \dots {}^5 A_6 (q_6) {}^6 A_E \tag{8}$$

Alternatively, (8) can be expressed by the form (9)

$${}^d A_E ({}^d p_E) = {}^0 A_d^{-1} {}^0 A_1 (q_1) {}^1 A_2 (q_2) \dots {}^5 A_6 (q_6) {}^6 A_E \tag{9}$$

The elements of the left side (9) are functions of the operational coordinate vector p (4). The elements of the right side (9) are functions of the joint coordinate vector q (1).

Direct kinematic computation is performed to determine position, velocity, and acceleration of the tool with respect to the workpiece, expressed to the workpiece frame. Positions, velocities, and accelerations of the joint variables are able to be measured by sensors. The right side of (9) are determined completely due to the joint variables are determined. Solving equations (9) to find the operational positions, velocities and accelerations of the tool with respect to the workpiece, expressed to the workpiece frame.

From manipulating requirements, motion of the end-effector is determined, inverse kinematic computation is carried out to determine the joint coordinates and its derivative, that means motions of the links are determined to meet the required cutting motion.

From (9), obtained the nonlinear algebraic equations (10).

$$f(q, p) = 0 \tag{10}$$

$$f = [f_1, \dots, f_6]^T \tag{11}$$

With the equations (10), in inverse kinematic problem, the variables are the joint coordinates (1), the parameters varying by time are position of the tool with respect to the machining surface, which is expressed by the operational coordinates p (4).

While conducting milling process, the cutter moves so as to the cutting point of the tooth tracks along the tool path on the machining surface. According to the method of matching trihedrons [8], in the case of form-shaping milling a complicated surface, the workpiece trihedron and the tool trihedron match together to meet the manufacturing demands. Therefore, the operational coordinates (4) are determined by the parameters of the workpiece surface of the tool path ${}^d x_{fi}, {}^d y_{fi}, {}^d z_{fi}, {}^d \alpha_{fi}, {}^d \beta_{fi}, {}^d \eta_{fi}$. Solving (10) to computing (1) by (4) can be done by applying the method Newton-Raphson.

According to material removal engineering in implementation, it is required to determine velocity and angular velocity of the tool on the tool path. This enables computing derivatives of the operational coordinates (4), that means (12) and (13) are determined.

$$\dot{p} = [{}^d \dot{x}_E, {}^d \dot{y}_E, {}^d \dot{z}_E, {}^d \dot{\alpha}_E, {}^d \dot{\beta}_E, {}^d \dot{\eta}_E]^T \tag{12}$$

$$\ddot{p} = [{}^d \ddot{x}_E, {}^d \ddot{y}_E, {}^d \ddot{z}_E, {}^d \ddot{\alpha}_E, {}^d \ddot{\beta}_E, {}^d \ddot{\eta}_E]^T \tag{13}$$

Carrying out the first derivative of (10) with respect to time t (14):

$$J_q \dot{q} = J_p \dot{p} \tag{14}$$

$$J_q = \frac{\partial f}{\partial q}; \quad J_p = -\frac{\partial f}{\partial p} \tag{15}$$

Obtaining the joint velocities, which are expressed by the first derivative of the joint coordinates (16)

$$\dot{q} = J_q^{-1} J_p \dot{p} \tag{16}$$

Carrying out the first derivative of (14) with respect to time t (17):

$$\dot{J}_q \dot{q} + J_q \ddot{q} = \dot{J}_p \dot{p} + J_p \ddot{p} \tag{17}$$

Obtaining the joint accelerations, which are expressed by the second derivative of the joint coordinates (18)

$$\ddot{q} = J_q^{-1} [\dot{J}_p \dot{p} + J_p \ddot{p} - \dot{J}_q \dot{q}] \tag{18}$$

III. ROBOT'S DIFFERENTIAL EQUATION OF MOTION

The paper analyses a serial robot, which have 6 degrees of freedom, employing in milling process to perform form-shaping workpiece surfaces. Figure 1 shows kinematic diagram of the robot that consist of 6 movable links connecting to the fixed base and a clamping table, which clamps the workpieces. The links of robot are notated by LK0 (the fixed link), LK1, LK2, ..., LK6 (the movable links) respectively, in which LK6 is the end-effector. The clamping table is notated by B.

The Lagrange equations of the robot in matrix form can be expressed as follows (19).

$$M(q)\ddot{q} + C(q, \dot{q}) + G(q) + Q = U \tag{19}$$

Here:

$M(q)$ – is the mass matrix, which is computed as (20). In (20), m_i is the mass of link i ; J_{Ti} is the Jacobian matrix of the coordinate vector of the center of mass of link ${}^0 r_{ci}$ with respect to the joint coordinates (21); J_{Ri} is the rotation Jacobian matrix of the angular velocity vector of link i with respect to the derivatives of joint coordinates (22); ${}^{ci} \Theta_{ci}$ is the inertia tensor of link i about C_i , expressed in the frame which is attached to C_i .

$$M(q) = \left[\sum_{i=1}^6 (J_{Ti}^T m_i J_{Ti} + J_{Ri}^T {}^{ci} \Theta_{ci} J_{Ri}) \right]_{6 \times 6} \tag{20}$$

$$J_{Ti} = \frac{\partial {}^0 r_{ci}}{\partial q} \tag{21}$$

$$J_{Ri} = \frac{\partial {}^i \omega_i}{\partial \dot{q}} \tag{22}$$

The coordinate vector of the center of mass of link ${}^0 r_{ci}$, the angular velocity vector of link ${}^i \omega_i$ are computed by transformation matrices from kinematic problem.

$C(q, \dot{q})$ - is the general force vector of coriolis and centrifugal forces (23), (24), (25).

$$C(q, \dot{q}) = [c_1, c_2, \dots, c_6]^T \tag{23}$$

$$c_j = \sum_{k,l=1}^6 (k,l;j) \dot{q}_k \dot{q}_l \tag{24}$$

$$(k,l;j) = \frac{1}{2} \left(\frac{\partial m_{kj}}{\partial q_l} + \frac{\partial m_{lj}}{\partial q_k} - \frac{\partial m_{kl}}{\partial q_j} \right) \tag{25}$$

With (k,l;j) is Christofel notation.

G(q) – is the vector of general forces of gravitational forces (26), (27).

$$G(q) = [g_1, g_2, \dots, g_6]^T \tag{26}$$

$$g_j = \frac{\partial \Pi}{\partial q_j}, \quad \Pi = \sum_{i=1}^n \Pi_i, \quad \Pi_i = m_i g z_{ci} \tag{27}$$

U – is the vector of general forces of driving forces (28), (29).

$$U = [U_1, U_2, \dots, U_6]^T \tag{28}$$

$$U_i = \tau_i \tag{29}$$

Here, τ_i is the driving force (or torque) of joint i (for prismatic joint, τ_i is force and for revolute joint, τ_i is torque).

Q(q) – is the vector of general forces and torques of none gravitational forces. The none gravitational forces include acting forces, friction forces, and the elements of cutting forces which cause by the workpiece surface acting on the tool at the contacting point. In this paper, in order to analysis effect of cutting forces, so we only consider the general force Q of the cutting forces.

The cutting force vector that generated by the workpiece surface acting on the tool is notated by F_c , corresponding to general force Q(q), computed by (30).

$$Q(q) = J_{F_c}^T F_c \tag{30}$$

Here, J_{F_c} is the Jacobian matrix of the vector 0r_E , which is the locating vector of the applying point of the force F_c with respect to the coordinate vector q (1). Matrix J_{F_c} is computed by (31).

$$J_{F_c} = \frac{\partial {}^0r_E}{\partial q} \tag{31}$$

IV. MILLING FORCES

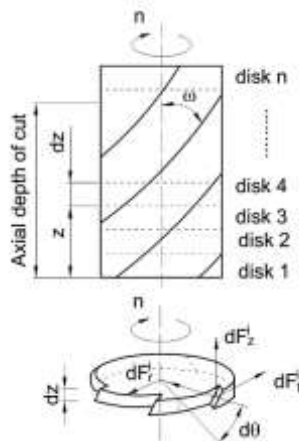


Figure 2. Cutting force expression of the flute icorresponding to an elemental disk dz

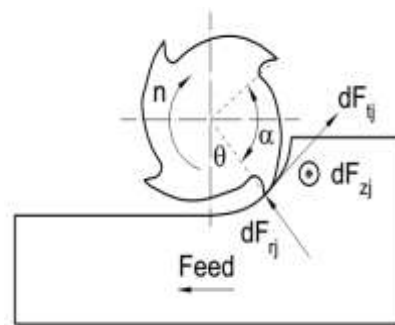


Figure 3. Cross-sectional view of an end mill showing differential forces

The cutting forces in milling process are determined by empirical formulas corresponding to specific engineering processes. There are a number of parameters and factors that affect to cutting forces such as: depth of cut t, feed rate s, spindle speed n, width of cut B, etc. From the mechanical model, the milling forces is determined by the model of interactive contaction between the tool and the workpiece surface. Beside that, material removal motion (form-shaping motion) of the cutter also affects to the parameters in the equations that determine cutting forces. So that, corresponding to a certain cutter, the geometric shape of cutter leads to the model of interactive contaction between the workpiece and the cutter.

The paper analyses the case that an end mill performs a down milling process. The mechanical model that describes interaction between the tool and the workpiece surface, the cutting force elements and engineering parameters, Figure 2 and 3.

Milling forces are generated at the contacting area of the cutter and workpiece. The contacting area has complicated spatial shape, depends on the structure and arrangement of the flutes on the cutter. Consequently, the milling forces are distributed spatial forces, so it is hard to calculate accurately cutting forces. To calculate approximately the cutting force values, the cutter is divided into a number of very thin disks by planes that perpendicular to the axis of the cutter, forming elemental disks that have thickness dz , Figure 2 [11-14]. Milling forces of a elemental disk is formulated, Figure 3, and the resultant forces are integrals of milling forces of the whole depth of cut. According to [11-14], cutting force elements corresponding to the flute j of the elemental disk dz is expressed by (32).

$$\begin{cases} dF_{tj}(\theta, z) = (K_{tc} a_j(\theta_j(z)) + K_{te}) dz \\ dF_{rj}(\theta, z) = (K_{rc} a_j(\theta_j(z)) + K_{re}) dz \\ dF_{aj}(\theta, z) = (K_{nc} a_j(\theta_j(z)) + K_{ne}) dz \end{cases} \quad (32)$$

In which:

dF_{tj} , dF_{rj} , dF_{aj} – are elemental cutting forces of the flute j in tangential, radial and axial directions respectively.

K_{tc} , K_{rc} , K_{nc} – milling force coefficients in tangential, radial and axial directions for linear force model.

K_{te} , K_{re} , K_{ne} – Cutting-edge coefficients in tangential, radial and axial directions for the linear force model.

$a_j(\theta, z)$ - chip thickness of the flute j (33):

$$a_j(\theta, z) = s_t \sin(\theta_j(z)) \quad (33)$$

s_t - feed rate: mm/tooth/rev.

$\theta_i(z)$ – the immersion angle changes along the axial direction (34)

$$\theta_j(z) = \theta(t) + (j-1)\alpha - k_\beta z; \quad \theta(t) = \frac{\pi n}{30} t; \quad k_\beta = \frac{tg\beta}{R} \quad (34)$$

α - the angular between the two consecutive flutes (35).

$$\alpha = \frac{2\pi}{N} \quad (35)$$

N – number of flutes of the cutter.

n – cutting tool speed (rpm).

β - helix angle of the cutting tool edges.

R – radius of the cutter, D – diameter of the cutter.

From Figure 3, selecting x axis in tangential direction, y axis in perpendicular direction of the tool path at the cutting point, z axis in the axial of the cutter, the elemental forces dF_{xj} , dF_{yj} , dF_{zj} in x , y , z directions applying on the flute j of the disk dz can be described(36)

$$\begin{bmatrix} dF_{xj}(\theta_j(z)) \\ dF_{yj}(\theta_j(z)) \\ dF_{zj}(\theta_j(z)) \end{bmatrix} = \begin{bmatrix} -\cos\theta_j(z) & -\sin\theta_j(z) & 0 \\ \sin\theta_j(z) & -\cos\theta_j(z) & 0 \\ 0 & 0 & 1 \end{bmatrix} \begin{bmatrix} dF_{tj}(\theta, z) \\ dF_{rj}(\theta, z) \\ dF_{aj}(\theta, z) \end{bmatrix} \quad (36)$$

Integrating by the elemental forces (36), obtained cutting forces acting on the flute j of cutter (37)

$$F_{kj}(\theta_j(z)) = \int_{z_{j1}}^{z_{j2}} F_{kj}(\theta_j(z)) dz; \quad k=x,y,z \quad (37)$$

Here: $z_{j1}(\theta_j(z))$, $z_{j2}(\theta_j(z))$ are under and upper limitation of the cutting flute j .

From (34), obtained $d\theta_j(z) = -k_\beta dz$, so cutting forces of the flute j (38) [12]

$$\left. \begin{aligned}
 F_{xj}(\theta_j(z)) &= \left\{ \begin{aligned}
 &\frac{S_t}{4k_\beta} \left[-K_{tc} \cos 2\theta_j(z) + K_{rc} \left[2\theta_j(z) - \sin 2\theta_j(z) \right] \right] \\
 &+ \frac{1}{k_\beta} \left[K_{te} \sin \theta_j(z) - K_{re} \cos \theta_j(z) \right]
 \end{aligned} \right\} \left. \begin{aligned}
 &z_{j2}(\theta_j(z)) \\
 &z_{j1}(\theta_j(z))
 \end{aligned} \right\} \\
 F_{yj}(\theta_j(z)) &= \left\{ \begin{aligned}
 &\frac{-S_t}{4k_\beta} \left[K_{tc} \left[2\theta_j(z) - \sin 2\theta_j(z) \right] + K_{rc} \cos 2\theta_j(z) \right] \\
 &+ \frac{1}{k_\beta} \left[K_{te} \cos \theta_j(z) - K_{re} \sin \theta_j(z) \right]
 \end{aligned} \right\} \left. \begin{aligned}
 &z_{j2}(\theta_j(z)) \\
 &z_{j1}(\theta_j(z))
 \end{aligned} \right\} \\
 F_{zj}(\theta_j(z)) &= \left\{ \frac{1}{k_\beta} \left[K_{nc} S_t \cos \theta_j(z) - K_{ne} \theta_j(z) \right] \right\} \left. \begin{aligned}
 &z_{j2}(\theta_j(z)) \\
 &z_{j1}(\theta_j(z))
 \end{aligned} \right\}
 \end{aligned} \right\} \quad (38)$$

The total cutting forces of all flutes at the time that corresponds to the immersion angle θ are computed by (39)

$$F_x(\theta) = \sum_{j=1}^N F_{xj}; \quad F_y(\theta) = \sum_{j=1}^N F_{yj}; \quad F_z(\theta) = \sum_{j=1}^N F_{zj} \quad (39)$$

V. NUMERICAL SIMULATIONS

Numerical computation is carried out with the case of robot perform milling form-shaping of a workpiece surface, shows in Figure 4.

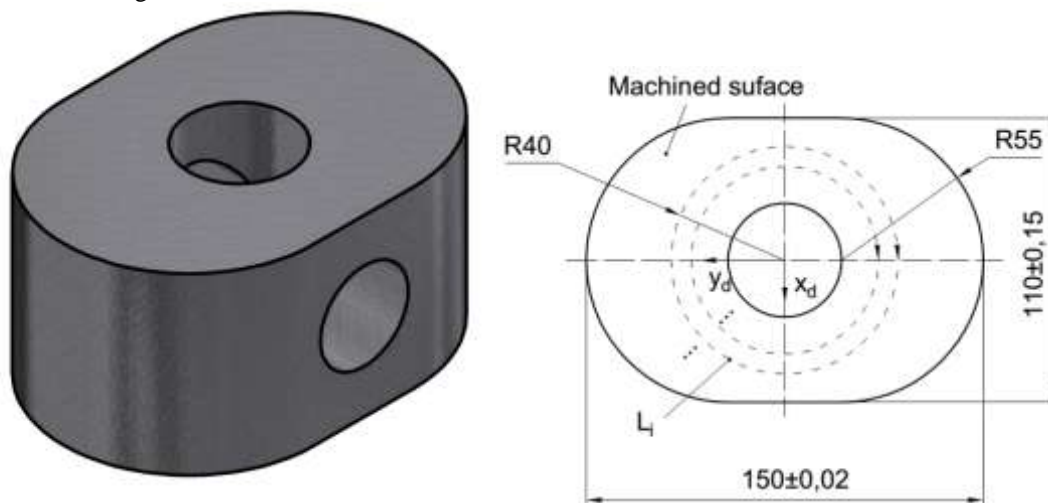


Figure 4. The workpiece and the form - shaping path

The machining robot model is obtained from ABB- robot IRB 6660.

Geometric and kinematic parameters are presented in Table 3. The other parameters, such as mass, inertial tensor, center of mass, etc, are not presented because of its cumbersome expression.

Table 3: Kinematic parameters of the robot

a_1	d_1	a_2	a_3	d_4	d_6	6x_E	6y_E	6z_E	${}^6\alpha_E$	${}^6\beta_E$	${}^6\eta_E$
300	514,5	700	280	1060,24	377	0	0	0	π	$\pi/2$	0

Units of notation in Table 3: Length – mm, n – rmp, feed rate S_v -mm/tooth/rev.

The workpiece parameters and cutting process parameters are presented in Table 4.

Table 4: Workpiece, cutting process parameters and coefficients

	Materials	h	S_v	n	K_{tc}	K_{rc}	K_{nc}	K_{re}	K_{te}	K_{ne}
1	Ti ₆ AL ₄ V	0.5	0,1	1000	1825	770	735	29.7	55.7	1.8
2	Ti ₆ AL ₄ V	0.5	0,1	1000	1698	438	591	24.7	42.9	5.5

Using the end-milling cutter that have 12.7mm diameter, two flute, helix angle $\beta=30^{\circ}$, the start and exit angles are 90° and 180° respectively $\theta_{st}=\pi/2$, $\theta_{ex}=\pi$.

Computing data for dynamics problem is conducted following the presented content, for a milling cycle along the tool path L, which is a haft of a circle, radius 40mm, figure 4

The computing and expressing results of the tool path with respect to the workpiece frame is showed in Figure 5. Figure 6 is the graph of the operational coordinates that expresses the form-shaping motion of robot. Due to the machining plane are planar and the plane of the workpiece frame coincides with the plane of the milling plane, so the operational coordinates in z_d direction and rotating about axes x_d , y_d are equal to zero.

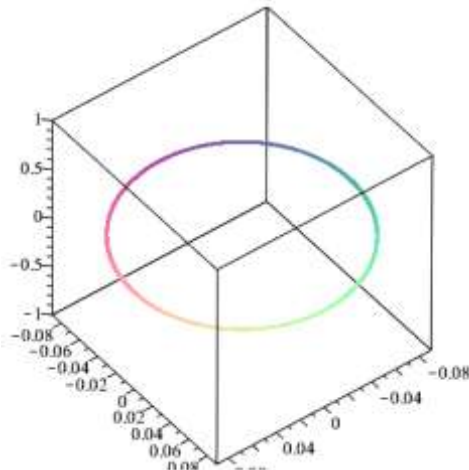


Figure 5. The form-shaping path

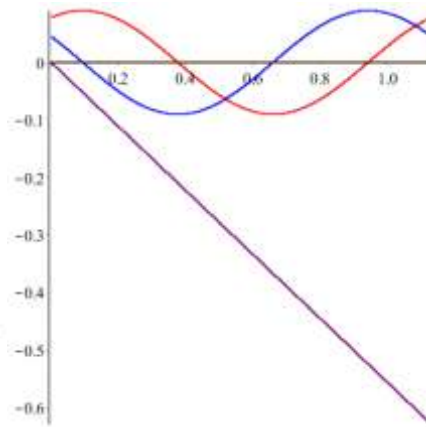


Figure 6. Operational coordinates

The joint positions and velocities are computed in the trajectory planning problem, and expressed in Figure 7,8.

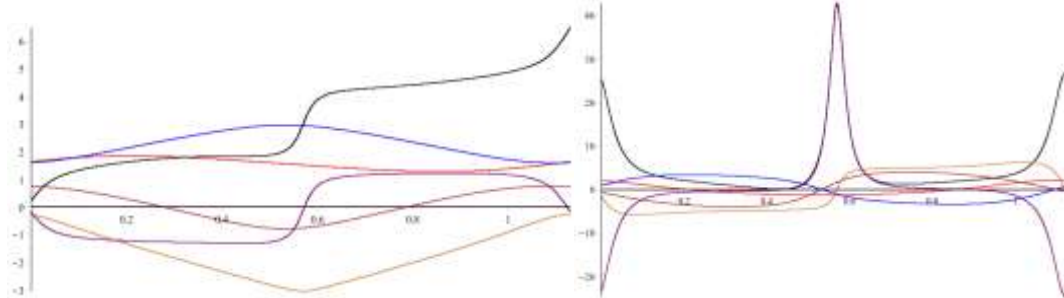


Figure 7. Joint coordinates Figure 8. Joint velocities

Figure 9 depicts part of cutting force graph that calculated for two cases with the cutting coefficients referencing from [16].

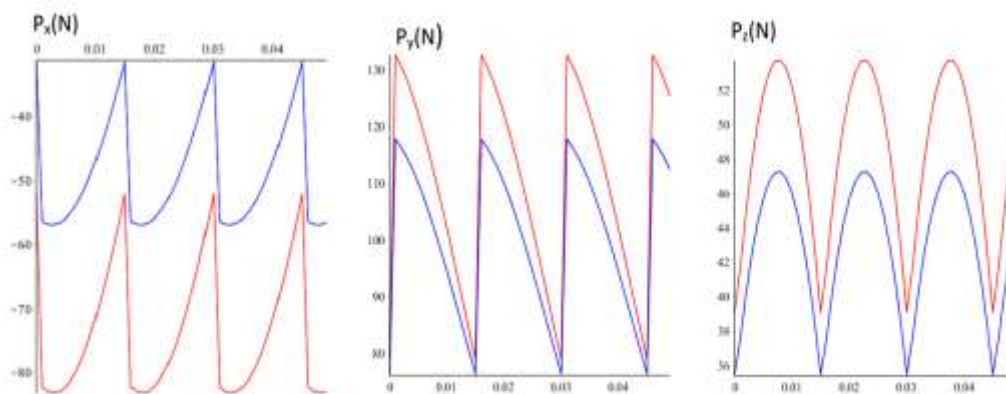


Figure 9. Cutting forces in the trihedron frame: red- case 1, blue-case 2

The results of solving dynamic problem are shows in Figure 10. Figure 10 is part of graph that compares the obtained form-shaping motion corresponding to cutting forces showing in Figure 9. The results enables conclusion as follows:

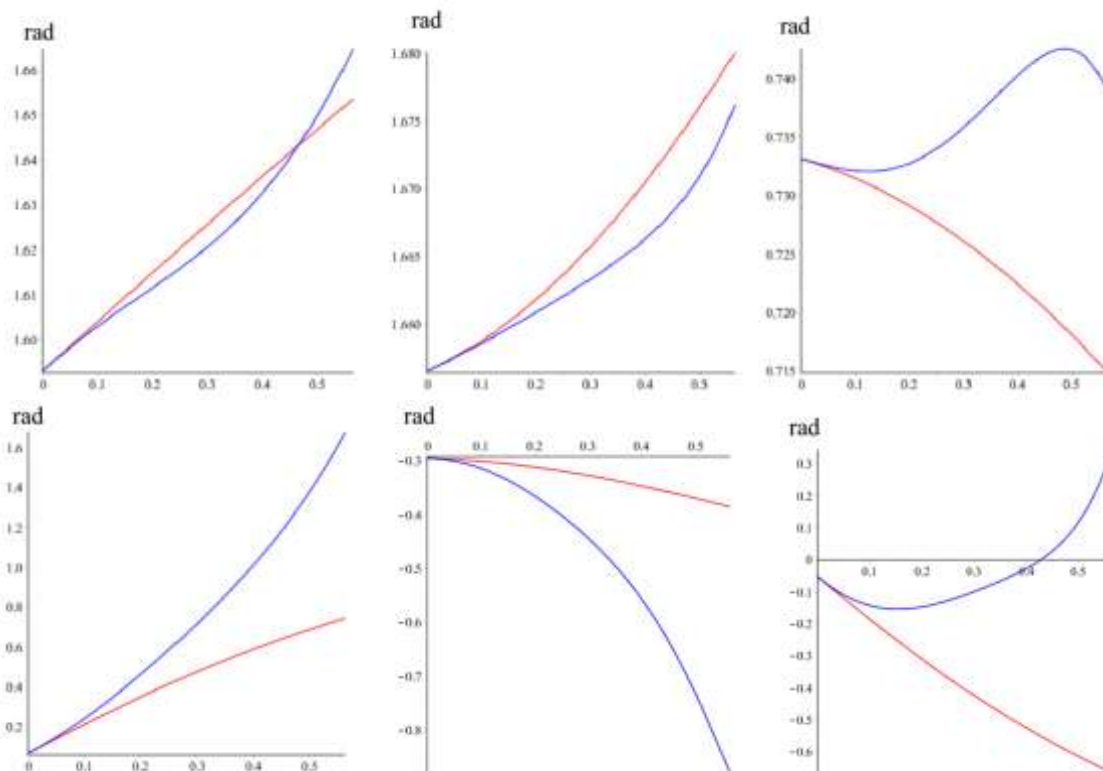


Figure 10. Driving forces: red-withdraw vibration, blue-under vibration

Cutting force calculations basing on empirical formulas have remarkable errors, depending on coefficient selections.

With different calculations and parameter selections of cutting forces lead to different approximate results, so that the motion of robot will be existed deviation under effect of cutting forces.

To the next study of employing robot in machining process is control problem. When applying the dynamic model to design controllers for robot, the control forces is computed with cutting force errors, as a result, the obtained motion will have deviations.

VI. CONCLUSIONS

This paper presents the results of kinematic and dynamic modelling of robots in form-shaping milling process, by utilizing the transformation coordinates and the homogeneous transformation matrices.

The applied algorithms enable computing and programing to derive and solve kinematic and dynamic equations, even robot kinematic structures have a large number of degrees of freedom, and cutting forces calculate and express complicatedly.

The results of solving direct dynamic problem show accuracy of the form-shaping motion, and the milling accuracy is affected by cutting forces.

The study results indicate that it is necessary to find out solutions to guarantee accuracy of form-shaping motion, by calculating precisely cutting forces;calibarating, eliminating or minimizing errors of cutting forces.

REFERENCES

- [1]. Appleton E, Williams DJ - Industrial robot applications. HALSTED PRESS, New York (1987), 229 pags.
- [2]. Wei Ji, Lihui Wang: Industrial robotic Machining: A review, The International Journal of Advanced manufacturing Technology. September 2011, pp. 1-17.
- [3]. John Pandremenos, Christos Doukas, Panagiotis Stavropoulos, George Chryssolouris-Machining with robots: a critical review. Proceedings of DET2011 7th International Conference on Digital Enterprise Technology, Athens, Greece, 28-30 September 2011.
- [4]. Iglesias I, Sebastián M A, Aresc J E - Overview of the state of robotic machining: Current situation and future potential. ScienceDirect, Procedia Engineering 132 (2015) 911 – 917.
- [5]. Zengxi Pan, Hui Zhang - Robotic machining from programming to process control: a complete solution by force control. Industrial Robot: An International Journal. Vol. 35(5), 2008, pp.400-409.
- [6]. LejunCena and Shreyes N. Melkote. - Effect of Robot Dynamics on the Machining Forces in Robotic Milling. ScienceDirect. 45th SME North American Manufacturing Research Conference, NAMRC 45, LA, USA 2017, pp. 486-496.
- [7]. GrzegorzGołda, Adrian Kampa. - Modelling of Cutting Force and Robot Load During Machining. Advanced Materials Research. Vol. 1036, pp. 715-720.

- [8]. Phan Bui Khoi, Ha Thanh Hai. Investigation of kinematics and motion planning for mechanical machining robots. Proceedings of the National Conference of Engineering Mechanics, Vol. 2, (2015), pp. 407-418 (In Vietnamese).
- [9]. Phan Bui Khoi, Ha Thanh Hai. Robot dynamics in mechanical processing. Proceedings of the National Conference of Engineering Mechanics, Vol. 2, (2015), pp. 419-427 (In Vietnamese).
- [10]. Phan Bui Khoi, Ha Thanh Hai. Force analysis of a robot in machining process. Proceeding of National conference on machines and mechanisms, (2015), pp. 346-359.
- [11]. Abele, E., et al. "Prediction of the tool displacement for robot milling applications using coupled models of an industrial robot and removal simulation." Proc. CIRP 2nd Inter Conf on Process Machine Interactions, Vancouver, Canada. 2010.
- [12]. Budak, Erhan. "Analytical models for high performance milling. Part I: Cutting forces, structural deformations and tolerance integrity." International Journal of Machine Tools and Manufacture 46.12-13 (2006): 1478-1488.
- [13]. Adem, Khaled AM. "Effects of machining system parameters and dynamics on quality of high-speed milling." PhD diss., University of Missouri-Columbia, 2013.
- [14]. Altintas, Y., M. Eynian, and H. Onozuka. "Identification of dynamic cutting force coefficients and chatter stability with process damping." CIRP annals 57.1 (2008): 371-374.
- [15]. Vosniakos, George-Christopher, and Elias Matsas. "Improving feasibility of robotic milling through robot placement optimisation." Robotics and Computer-Integrated Manufacturing 26.5 (2010): 517-525
- [16]. Budak, E., Y. Altintas, and E. J. A. Armarego. "Prediction of milling force coefficients from orthogonal cutting data." Journal of Manufacturing Science and Engineering 118.2 (1996): 216-224.

Ha Thanh Hai" Effect of Cutting Forces on the Form-Shaping Motion in Robotic Milling"
International Journal of Humanities and Social Science Invention(IJHSSI), vol. 8, no. 7, 2019,
pp. 176-185